Research Article | Vol. 24, No. 15 | 25 Jul 2016 | OPTICS EXPRESS 17200

Optics EXPRESS

Evaluation of the accuracy of BOTDA systems based on the phase spectral response

ALEXIA LOPEZ-GIL,[1,*] MARCELO A. SOTO,[2] XABIER ANGULO-VINUESA,[1] ALEJANDRO DOMINGUEZ-LOPEZ,[1] SONIA MARTIN-LOPEZ,[1] LUC THÉVENAZ[2] AND MIGUEL GONZALEZ-HERRAEZ[1]

[1] *Departamento de Electrónica, Universidad de Alcalá, Escuela Politécnica Superior, Campus Universitario s/n, 28805 Alcalá de Henares, Spain*
[2] *EPFL Swiss Federal Institute of Technology, Institute of Electrical Engineering, SCI STI LT, Station 11, CH-1015 Lausanne, Switzerland*
alexia.lopez@uah.es

Abstract: We evaluate the Brillouin frequency shift (BFS) determination error when utilizing the Brillouin phase spectrum (BPS) instead of the Brillouin gain spectrum (BGS) in BOTDA systems. Systems based on the BPS perform the determination of the BFS through a linear fit around the zero de-phase frequency region. An analytical expression of the error obtained in the BFS determination as a function of the different experimental parameters is provided and experimentally validated. The experimental results show a good agreement with the theoretical predictions as a function of the number of sampling points, signal-to-noise ratio (SNR) and Brillouin spectral linewidth. For an equal SNR and linewidth, the phase response only provides a better BFS estimation than the gain response when the fit is performed over a restricted frequency range around the center of the spectral profile. This may reduce the measurement time of specific BOTDA systems requiring a narrow frequency scanning. When the frequency scan covers most of the Brillouin spectral profile, gain and phase responses give very similar estimations of the BFS and the BPS offers no crucial benefit.

OCIS codes: (060.2310) Fiber optics; (060.2370) Fiber optics sensors; (290.5900) Scattering, stimulated Brillouin; (060.4370) Nonlinear optics, fibers.

References and Links

1. T. Horiguchi and M. Tateda, "BOTDA-nondestructive measurement of single-mode optical fiber attenuation characteristics using Brillouin interaction: theory," J. Lightwave Technol. **7**(8), 1170–1176 (1989).
2. G. P. Agrawal, *Nonlinear Fiber Optics* (Academic, 2007), Ch. 9.
3. M. Nikles, L. Thévenaz, and P. Robert, "Brillouin gain spectrum characterization in single-mode optical fibers," J. Lightwave Technol. **15**(10), 1842–1851 (1997).
4. M. A. Soto and L. Thévenaz, "Modeling and evaluating the performance of Brillouin distributed optical fiber sensors," Opt. Express **21**(25), 31347–31366 (2013).
5. J. Urricelqui, A. Zornoza, M. Sagues, and A. Loayssa, "Dynamic BOTDA measurements based on Brillouin phase-shift and RF demodulation," Opt. Express **20**(24), 26942–26949 (2012).
6. M. Dossou, D. Bacquet, and P. Szriftgiser, "Vector Brillouin optical time-domain analyzer for high-order acoustic modes," Opt. Lett. **35**(22), 3850–3852 (2010).
7. X. Lu, M. A. Soto, M. Gonzalez-Herraez, and L. Thévenaz, "Brillouin distributed fibre sensing using phase modulated probe," Proc. SPIE **8794**, 87943P (2013).
8. X. Tu, Q. Sun, W. Chen, M. Chen, and Z. Meng, "Vector brillouin optical time-domain analysis with heterodyne detection and IQ demodulation algorithm," IEEE Photonics J. **6**(2), 6800908 (2014).
9. A. Lopez-Gil, X. Angulo-Vinuesa, A. Dominguez-Lopez, S. Martin-Lopez, and M. Gonzalez-Herraez, "Exploiting nonreciprocity in BOTDA systems," Opt. Lett. **40**(10), 2193–2196 (2015).
10. A. Lopez-Gil, X. Angulo-Vinuesa, A. Dominguez-López, S. Martin-Lopez, and M. Gonzalez-Herraez, "Simple BOTDA temperature sensor based on distributed Brillouin phase-shift measurements within a Sagnac interferometer," Proc. SPIE **9634**, 96346L (2015).
11. A. Lopez-Gil, X. Angulo-Vinuesa, A. Dominguez-Lopez, S. Martin-Lopez, and M. Gonzalez-Herraez, "Simple baseband method for the distributed analysis of Brillouin phase-shift spectra," IEEE Photonics Technol. Lett. **28**(13), 1379–1382 (2016).

#265403 http://dx.doi.org/10.1364/OE.24.017200
Journal © 2016 Received 18 May 2016; revised 3 Jul 2016; accepted 7 Jul 2016; published 20 Jul 2016

Optics EXPRESS

12. X. Angulo-Vinuesa, A. Lopez-Gil, A. Dominguez-Lopez, J. L. Cruz, M. V. Andres, S. Martin-Lopez, and M. Gonzalez-Herraez, "Simultaneous gain and phase profile determination on an interferometric BOTDA," Proc. SPIE **9634**, 963419 (2015).
13. E. Lichtman, R. G. Waarts, and A. A. Friesem, "Stimulated Brillouin scattering excited by a modulated pump wave in single-mode fibers," J. Lightwave Technol. **7**(1), 171–174 (1989).
14. A. Fellay, L. Thévenaz, M. Facchini, M. Niklès, and P. Robert, "Distributed sensing using stimulated Brillouin scattering: towards ultimate resolution," in *12th International Conference on Optical Fiber Sensors*, OSA Technical Digest Series (Optical Society of America, 1997), paper OWD3.
15. P. H. Richter, "Estimating errors in least-squares fitting," Telecommun. Data Acquisition Prog. Rep. **42**(122), 107–137 (1995).
16. L. Thévenaz, S. F. Mafang, and J. Lin, "Effect of pulse depletion in a Brillouin optical time-domain analysis system," Opt. Express **21**(12), 14017–14035 (2013).

1. Introduction

The use of Brillouin-based distributed fiber sensors has increased considerably in the past few years thanks to their ability to sense strain and temperature in a distributed way over many tens of kilometers with meter-scale resolutions. Distributed Brillouin sensors therefore provide continuous monitoring of tens of thousands of sensing points along a single optical fiber cable. Brillouin optical time domain analysis (BOTDA) systems [1] have consequently attracted great interest in fields such us pipeline leakage monitoring and civil structure monitoring, where a large number of sensing points is typically required.

BOTDA systems make use of the well-known physical phenomenon called stimulated Brillouin scattering (SBS) [2]. SBS in optical fibers couples light among two counter-propagating light waves through an acousto-optic process. This means that when an intense coherent pump wave (at a frequency v_0) propagates along an optical fiber, SBS manifests by inducing counter-propagating frequency-shifted narrowband amplification and attenuation processes at frequencies $(\nu_0 - \nu_B)$ and $(\nu_0 + \nu_B)$, respectively. The quantity v_B is known as the Brillouin frequency shift (BFS) of the fiber, and depends on the refractive index and the acoustic velocity in the fiber. The gain and loss SBS curves follow a Lorentzian distribution (Brillouin gain/loss spectrum – BGS/BLS) subject to an associated phase response, called the Brillouin phase spectrum (BPS), depicted by the dashed lines in Fig. 1. Both spectra, i.e. BGS and BPS, are centered on the BFS of the fiber, and experience a spectral shift with a linear dependence on strain ε and temperature T. This dependence of the BFS makes SBS suitable for distributed sensing, thus enabling a sensing system that can provide a longitudinal profile of these physical quantities.

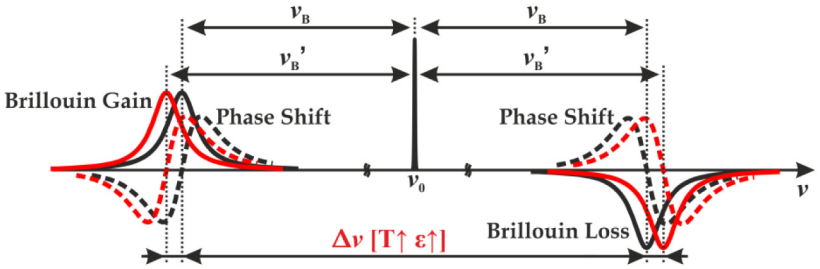

Fig. 1. Schematic representation of the BGS/BLS (gain - loss) and BPS (phase) including their dependence with increased strain $\mathcal{E}$ or temperature T.

In a conventional BOTDA configuration, a pulsed pump wave is used to induce Brillouin gain over a continuous-wave probe signal, which is measured and then analyzed as a function of the time-of-flight of the pulse within the fiber. This scheme allows localizing the SBS interaction as a function of time and therefore performing position-resolved measurements of strain and temperature. The probe wave is typically obtained from the same master laser used for the pump by using a double-sideband modulation scheme (DSB). The pump-probe Brillouin spectral interaction is conventionally interrogated by scanning the probe modulation

Optics EXPRESS

frequency, so that a 3D map of the BGS along the fiber is obtained [3]. Then, by fitting a quadratic curve to the gain spectrum locally measured at each fiber position [4], a distributed profile of the BFS evolution along the fiber is obtained, and consequently any local temperature or strain variation can be detected in the fiber.

Since temperature and strain-induced BFS spectral changes result in equal frequency shifts of the peak amplitude of the BGS and the zero de-phase of the BPS, the Brillouin phase response can also be used as an alternative to the classical BGS to provide strain and temperature sensing [5]. Several techniques have been recently proposed to retrieve the longitudinal BFS profile by measuring the BPS along the fiber. For instance, techniques based on phase modulation make use of a complex coherent detection system employing high-bandwidth photo-detection [5–7] or IQ demodulation [8]. In contrast to these coherent methods, the use of a Sagnac interferometer within the sensing fiber of a standard BOTDA system (SI-BOTDA) has been recently proposed [9–11] to determine the distributed BPS feature using a conventional direct-detection scheme. One variant of the SI-BOTDA [12] provides simultaneous detection of the Brillouin gain and phase spectrum. Independently of the different features that all these implementations have, the BFS of the fiber is always retrieved by fitting a linear curve to the central spectral region of the BPS. This has allowed the implementation of reliable sensing systems based on the phase response of the SBS induced in the sensing fiber [5–12], instead of using the classical SBS gain response typically measured by conventional BOTDA sensors.

It is however still unclear under which conditions the linear fitting of the BPS provides better (or worse) accuracy to the BFS determination when compared to the use of the classical quadratic fitting over the BGS. In the literature, the performance of standard (gain/loss) BOTDA systems has been thoroughly analyzed and evaluated in terms of the best achievable error in the BFS determination [4]. However, to the best of our knowledge, a similar analysis has never been performed for the phase profile case. Comparisons presented in the literature could be highly influenced by the impact on the SNR from the different detection schemes, such as direct or coherent detection, and therefore a true comparison under similar measurement conditions is still missing in the literature.

In this paper we present a statistical analysis of the error produced when determining the BFS profile by employing BPS measurements. A mathematical expression for the BFS uncertainty as a function of different experimental parameters is proposed and experimentally validated. Theoretical and experimental results are also compared with the frequency uncertainty obtained by the classical quadratic fitting of the BGS under similar measurement conditions using a SI-BOTDA, i.e. considering the same scanning frequency range, frequency step, spatial resolution, and more importantly under the same SNR conditions. The results prove that, under conventional scanning conditions (scanning a spectral range comparable to the BGS spectral width $\Delta\nu_B$) and using a large enough number of scanned spectral points, the quadratic fitting of the BGS confidently provides a better accuracy than using a linear fitting over the BPS. However, the approach of using a linear fitting of the BPS can result in a better accuracy under very specific conditions, especially when a narrow frequency range has to be scanned around the BFS, enabling for instance very high-resolution or faster measurements.

2. Error in the BFS determination based on Brillouin phase spectral measurements

In this section, a statistical analysis is presented to estimate the frequency error in BOTDA systems when determining the BFS of the sensing fiber through the use of a linear fitting around the zero de-phase frequency of the BPS.

In a conventional BOTDA system, the determination of the associated temperature or strain variations is normally performed by estimating the center frequency position of the measured spectral gain profile, which is typically affected by additive white Gaussian noise. This maximum gain frequency ν_B is usually obtained by fitting the measured noisy BGS to a

Optics EXPRESS

parabolic polynomial curve, as represented in Fig. 2. In a normalized case, the gain exhibits a value of 1 at the BFS position and a value of 0.5 at a detuning of $\pm \Delta\nu_B/2$ from the BFS position. As the phase profile shifts its central frequency by the same amount as the BGS, it is also possible to determine the BFS by obtaining the frequency position at which the probe wave suffers no de-phase (see Fig. 2). The local phase response of the SBS interaction can be obtained from homodyne or heterodyne BOTDA measurements [5–12]. In any case, in a typical small gain case, the recovered phase profile is also affected by white Gaussian noise, and a fitting is convenient to recover the true zero-phase position. In this case, instead of using a second-order polynomial curve, a first-order polynomial curve (i.e. a straight line) is fitted to the BPS around the zero de-phase frequency. Ideally, the normalized phase response in this case exhibits a value of 0 at the BFS position and values of ± 0.5 at a detuning of $\pm \Delta\nu_B/2$ from the BFS position (see Fig. 2). The slope of the straight line that passes across these three points is thus $1/\Delta\nu_B$. It is important to notice that, unlike the quadratic fitting of the BGS, the strictly linear phase response region of the BPS is limited to an interval of the order of half the full-width at half-maximum (FWHM) of the BGS, representing the maximum spectral range to be fitted in the BPS. Nevertheless, we will compare both fittings for spectral spans up the FWHM of the BGS curve. This is actually fairly justified by the fact that the spectral profiles are no longer purely Lorentzian at spatial resolutions below ~5 m as a result of the convolution of the natural Lorentzian Brillouin with the pump pulse spectrum [13, 14]. Thus, at the usual meter-scale spatial resolutions, the central part of the effective gain profile turns out to be a generic bell-shaped distribution that is well represented by a plain parabolic function, and not so much well-represented with a pure Lorentzian. Equivalently, in the phase domain the phase curve linearizes substantially in the spectral range within the FWHM of the BGS, which means that a linear fit is better than a fit to the phase part of the Lorentzian gain.

An error in the frequency estimation of either the peak of the BGS or the zero de-phase of the BPS is typically produced due to the presence of noise in the measurements. Focusing our attention to the region in Fig. 2 where the fits are performed, it can be immediately noticed that the BPS presents the maximum slope in the center of its spectral profile where the BGS presents a vanishing slope, and vice versa. This intuitively suggests that the BGS fitting will give a very poor estimation when restricted over the central region – so in the strict vicinity of the peak gain – while the BPS can give an optimized estimation in the same region. Reversely, the estimation using the BPS does not really benefit from an enlarging of the fitting range while the BGS offers much improved conditions when the fitting range spans over the FWHM. The mathematical expressions deduced hereafter and the experimental validations fully confirm this intuition, giving moreover a quantitative comparison crucial to determine which approach will eventually result in the smallest error on the BFS determination.

In [4] a statistical analysis for estimating the frequency uncertainty in the BFS determination was presented for the conventional Brillouin gain/loss spectrum case. Here, by following a similar approach based on the error propagation of a least-square linear fit [15] of the Brillouin phase response curve, an equivalent mathematical expression is proposed for the BFS determination based on BPS measurements. Note that for the sake of simplicity, we will assume that the measurements are performed with a well-designed BOTDA sensor, which necessarily operates in a small-gain regime at metric spatial resolutions and is designed to minimize measurement distortions resulting from nonlocal effects [16]. In order to provide the same framework as used in [4], and thus to obtain a fairly comparable mathematical expression, the measured gain spectrum is normalized, so that its maximum gain amplitude equals 1. Note that under this condition the measurement noise σ in the time-domain traces turns out to be equal to the inverse of the SNR of the peak-frequency temporal trace, hence offering the possibility to link the quality of the measured time-domain traces with the measurand quality (i.e. with the frequency uncertainty in the BFS determination).

Optics EXPRESS

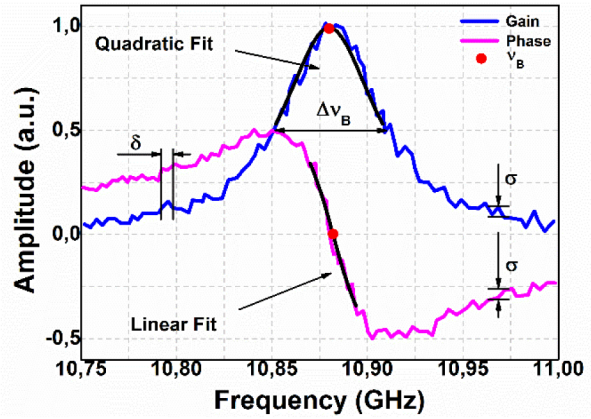

Fig. 2. Graphical representation of experimental gain and phase profiles obtained simultaneously through the SI-BOTDA presented in [12]. In the picture, the position of the BFS is represented with a red dot (at the maximum of the BGS and the zero-cross for the BPS measurement) as well as the most convenient mathematical fits to determine it; quadratic and linear for the gain and phase curves respectively. The relevant experimental parameters to determine the BFS determination error are also shown: frequency sampling step δ, gain FWHM $\Delta\nu_B$ and normalized noise σ.

In order to estimate the frequency error in the BFS determination using the BPS, let us consider that the central spectral region of the measured local Brillouin phase spectrum (at a given fiber position) is fitted by the following generic linear function:

$$y(x) = a\,x + b \tag{1}$$

where the coefficients a and b correspond to the slope and intercept of the fitted straight line, and are estimated from a least-square fitting procedure. Then, using those coefficients, the local BFS can be estimated as the frequency ν_B showing the zero de-phase, i.e. when $y(\nu_B) = 0$, leading to:

$$y(\nu_B) = a\nu_B + b = 0 \quad \Rightarrow \quad \nu_B = -\frac{b}{a} \tag{2}$$

Under standard measurement conditions, the time-domain traces are typically affected by additive white Gaussian noise and the error on the estimation of ν_B can be calculated from the errors induced in the estimation of the coefficients a and b as follows [4]:

$$\sigma_\nu^2 = \left|\frac{\partial \nu_B}{\partial a}\right|^2 \sigma_a^2 + \left|\frac{\partial \nu_B}{\partial b}\right|^2 \sigma_b^2 + 2\frac{\partial \nu_B}{\partial a}\frac{\partial \nu_B}{\partial b} cov_{a,b} \tag{3}$$

where σ_a^2 and σ_b^2 are the variances of the coefficients a and b respectively, and $cov_{a,b}$ is the covariance between a and b. Following the same strategy presented in [4], it is possible to set a condition in which the covariance term completely vanishes: this is the case when the spectral data points used in the linear fitting are uniformly and symmetrically distributed around the expected BFS. Practically this condition is easily met by performing several passes in the fitting process. Under this condition, the mathematical expressions for the factors σ_a^2 and σ_b^2 can be significantly simplified, so that by following the statistical analysis described in [4] and [15], the factors σ_a^2 and σ_b^2 can be written as:

$$\sigma_a^2 = \frac{12\sigma^2}{N\left(N^2-1\right)\delta^2} \tag{4}$$

Optics EXPRESS

$$\sigma_b^2 = \frac{\sigma^2}{N} \tag{5}$$

where N is the number of spectral points used in the fitting, σ^2 is the variance of the Gaussian noise affecting the measured traces, and δ is the frequency step used to scan the phase spectral response. Using Eqs. (3)-(5), the following expression for the error on the estimated local Brillouin frequency shift can be obtained:

$$\sigma_\nu^2 = \frac{\sigma^2}{a^2 N}\left[1 + \frac{12b^2}{a^2 N^2 \delta^2}\right] \tag{6}$$

where $N >> 1$ has been assumed. Note that the second term in Eq. (6) depends on the estimated coefficient b, which corresponds to the expected intercept of the fitted straight line. It should be reminded here that the assumption in our analysis is that the curves have zero horizontal and vertical offset. Since the situation here is to find the frequency ν_B that induces zero de-phase in the Brillouin response, the expected intercept b should be zero. This leads to a second term having in principle a negligible amplitude in comparison to the first term, which depends basically on the error in the estimation of the slope a of the fitted straight line. However, in general, the vertical offset term will not always be zero. This is actually a very important aspect to take into account when using a linear fitting, because any potential and unwanted offset impacting on the time-domain traces, as a result of the measurement process, will have a direct impact on the second term in Eq. (6), making it non-negligible and leading to high uncertainty in the BFS determination. Moreover, the impact of this second term will be larger for smaller measurement spans (smaller $N\delta$). This issue makes the use of a linear fitting less reliable from this point of view, especially when compared to the use of the conventional quadratic fitting, in which any spectrally-uniform offset in the measurements does not have any impact on the BFS determination. It is therefore important that BPS measurements are not biased by any offset, or that this offset is somehow corrected. In case of having a large measurement span, this offset could be corrected, for instance, by forcing that the integral of the data points scanning of the BPS is equal to zero (considering that the scanned spectral range is much larger than the FWHM, $\Delta\nu_B$). However, this may not be a valid procedure in all situations as in most cases the use of the BPS will only be convenient for reduced measurement spans. In such case, correcting the offset may be difficult or even impossible, and ensuring zero offset in the measurement scheme will be of utmost importance to avoid errors.

Anyway, to continue with our analysis, and considering the above-mentioned assumptions (zero vertical and horizontal offsets) that were also partially made for the BGS case (zero horizontal offset only, no impact of the vertical offset on the BFS estimation), the error in the BFS determination using a linear fitting of the Brillouin phase response can be reduced to:

$$\sigma_\nu^2 = \frac{\sigma^2}{a^2 N} \tag{7}$$

where a is the slope of the fitted straight line which is defined by the inverse of the FWHM of the BGS, so that $a = -1/\Delta\nu_B$. This way, the frequency error determined by the linear fit $\sigma_{\nu\text{-}linear}$ in Eq. (7) can be written as:

$$\sigma_{\nu-linear}(z) = \sigma(z)\Delta\nu_B\sqrt{\frac{1}{N}} = \frac{1}{SNR(z)}\Delta\nu_B\sqrt{\frac{1}{N}} \tag{8}$$

Note that this uncertainty depends on the measurement noise σ, the number of points N, and the Brillouin spectral width, which defines the slope of the straight line $a = -1/\Delta\nu_B$. Unlike the estimated error using a quadratic fitting [4], the expression in Eq. (8) does not depend on the frequency step used to scan the BPS. This can be explained by the fact that in the quadratic case the spectral range used to fit the BGS is essential to properly identify the

Optics EXPRESS

curvature of the polynomial curve, having in this way a direct impact on the estimation of the BFS error. In the case of the linear fitting, the spectral width is not an explicitly important parameter, and what really defines the error in the BFS estimation, besides the SNR, is the number of points used in the fitting and the slope of the fitted line (proportional to the inverse of the FWHM of the BGS). Again, it should be clear that the assumptions used imply no vertical or horizontal offset. In case of such an offset, an inevitable error appears which does indeed depend on the measurement step. This error grows as the step is reduced, as shown in Eq. (6).

In order to provide a fair comparison with the classical quadratic fitting of the BGS, the expression reported in [4] has to be presented using the same parameters as Eq. (8). According to [4], if $\Delta\nu_B$ is the Brillouin full-width at half maximum (FWHM) and δ the frequency sampling step (see Fig. 2), the frequency determination error for the quadratic $\sigma_{\nu\text{-}parabolic}$ fit of the BGS can be expressed as [4]:

$$\sigma_{\nu-parabolic}(z)=\sigma(z)\sqrt{\frac{3\delta\Delta\nu_B}{8\sqrt{2}(1-\eta)^{3/2}}} \tag{9}$$

where η is the fraction of the maximum peak level over which the quadratic fit is performed. For instance, when η equals 0.5, it means that the points involved in the quadratic fitting are within the FWHM or $\Delta\nu_B$. In the same way, if η = 1, just the peak position (a unique point) of the gain curve is selected, which means that no fitting can be performed, therefore raising the error to ∞, as validated by Eq. (9).

The use of this η variable is completely straightforward when dealing with a normalized gain curve, showing a minimum amplitude equal to 0 (no gain) and maximum gain normalized to 1, as described in [4]. In the case of using the BPS, η translates into an equivalent spectral range in the BPS to be fitted and can be expressed as a function of the number of points N, the frequency step δ and $\Delta\nu_B$ [4]:

$$\eta=1-\frac{N^2\delta^2}{2\Delta\nu_B{}^2} \overset{\xi=\frac{N\delta}{\Delta\nu_B}}{\Rightarrow} \eta=1-\frac{\xi^2}{2} \tag{10}$$

Note that η has now been re-defined as a function of the variable ξ, which is the measurement span $N\delta$ normalized to the BGS spectral width $\Delta\nu_B$. Using Eq. (10), it is possible to rewrite Eq. (9) as:

$$\sigma_{\nu-parabolic}(z)=\sigma(z)\frac{\Delta\nu_B{}^2}{2N\delta}\sqrt{\frac{3}{N}}=\sigma(z)\Delta\nu_B\frac{1}{2\xi}\sqrt{\frac{3}{N}} \tag{11}$$

Comparing Eq. (8) and Eq. (11) it is possible to point out that under the same experimental conditions (SNR, δ, $\Delta\nu_B$ and N), for small frequency sweeps $N\delta << \Delta\nu_B$, the error in the determination of the BFS becomes very high for the quadratic case (BGS) while it remains quite bounded in the linear case (BPS). As it was intuitively suggested and will come out explicitly from the later discussion on the results, this fact simply means that a quadratic fitting is very imprecise when performed over noisy points located in the close vicinity of the parabola center: in this case the curvature can be hardly discerned. Assuming the number of points N and the frequency step δ constant in the fitting process, Eqs. (8) and (11) shows a difference in behavior of both errors with $\Delta\nu_B$, being quadratic for the $\sigma_{\nu\text{-}parabolic}$ case and linearly dependent in the $\sigma_{\nu\text{-}linear}$ case. This simply indicates that for a constant fitting frequency range the points concentrate more in the center for larger $\Delta\nu_B$ and the quadratic fitting turns more rapidly imprecise. Experimental results using a SI-BOTDA will confirm this observation, as we will show in Section 3. It must be mentioned, however, that in a normal measurement procedure the frequency step δ is adapted to $\Delta\nu_B$ to cover a reasonable

Optics EXPRESS

spectral range to perform a fitting (i.e. the frequency step is adapted to the spectral width to cover roughly the same fraction of curve with the same number of points).

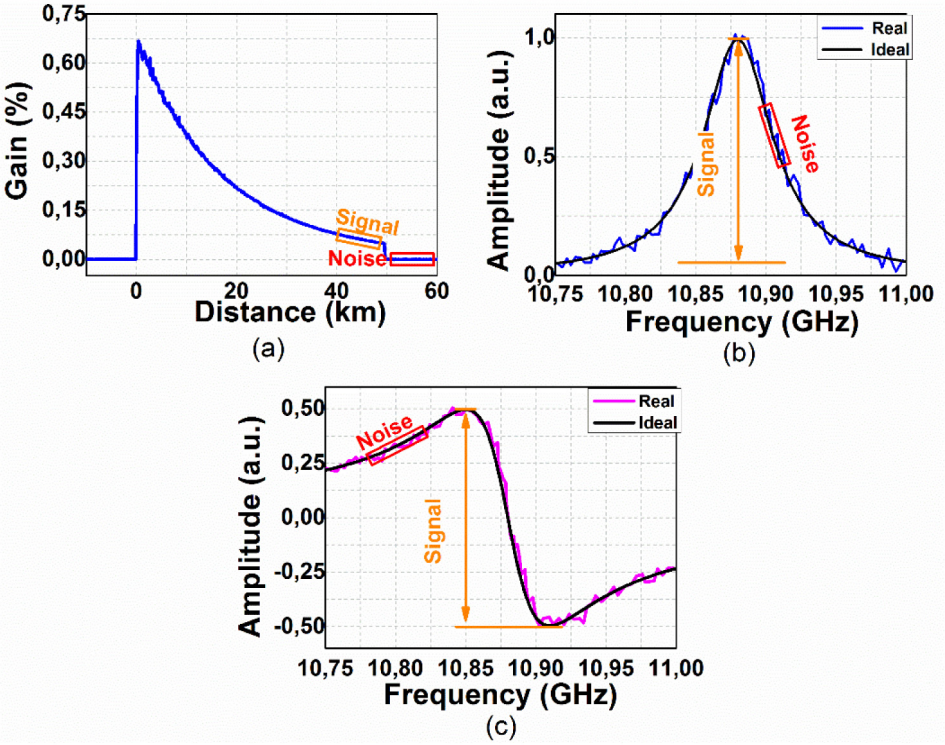

Fig. 3. Temporal normalized gain trace obtained with a standard BOTDA sensor. Noisy and ideal gain (b) and phase (c) profiles. In all cases, it has been defined the signal and the noise to calculate the SNR.

Even though in our experimental work [9–12] both gain and phase curves have the same SNR, as they are obtained from addition/subtraction from the same experimental measurements, it is necessary to define a general method to measure the SNR for both cases in case the methodology is tested independently for the BGS or BPS. Normally, in standard BOTDA systems, the SNR is obtained directly from the time domain trace measurements by analyzing, for the maximum gain frequency, the mean value of a given sampled point divided by its standard deviation. This is usually computed in the worst possible working conditions, which correspond to the end of the time-domain trace. In the usual working conditions (small gain), a first approximation indicates that it is sufficient to compute the ratio among the average amplitude of a flat region around maximum gain at the end of the fiber and the standard deviation outside the trace (see Fig. 3(a)). In the BGS domain (Fig. 3(b)), this procedure is essentially equivalent to analyzing the ratio among the maximum gain and the standard deviation of the spectral points. If there is no systematic error, the signal can be considered as the retrieved amplitude at maximum frequency and the noise as the standard deviation of the difference among an ideal theoretical trace (black trace) and the measured case (blue trace). This procedure can be equivalently applied to the phase case, analyzing the ratio among the peak-to-peak amplitude response (max-min of the BPS response) and the standard deviation of the spectral points, as shown in Fig. 3(c). By this mean, it is possible then to define a standard procedure to measure the SNR on any phase-measuring BOTDA. This SNR measurement procedure has been tested with the obtained experimental results and the values matched perfectly for both gain and phase cases.

Optics EXPRESS

3. Analysis and comparison of the error determination in the gain and phase cases

Equations (8) and (11) show the dependence of the error obtained when determining the BFS σ_v in the BGS and BPS cases as a function of the number of points employed in the fitting N, the frequency step (δ– only relevant in the quadratic case), the signal-to-noise ratio SNR and the Brillouin linewidth $\Delta\nu_B$. We will show now the evolution of both quadratic (Eq. (11)) and linear fitting errors (Eq. (8)) as a function of these quantities. To verify the above-described theory, we also provide experimental error data obtained from BGS and BPS measurements, both obtained from the same SI-BOTDA [9–12]. As mentioned previously, this scheme provides a simple baseband method for determining simultaneously the gain and phase profiles of the SBS interaction along the fiber. These measurements fit very well our purpose, since BGS and BPS profiles are obtained from simple addition and subtraction of two independent measurements [9–12]. This means that the gain and phase responses are obtained with the same SNR, and the comparison between the two cases can be fairly performed. Nevertheless, the conclusions of our study are absolutely general for any kind of phase-measuring BOTDA. In order to avoid any impact on the BFS determination, as mentioned previously, we need to ensure that the phase curve has zero vertical offset. To correct this offset, we have performed measurements with a large measurement span forcing that the integral of the data points scanning of the BPS is equal to zero. Once this is done, we have selected only a portion of this large measurement span depending on the number of measured frequency points N around the BFS that we need to analyze in each case.

First, we analyze the dependence of both errors $\sigma_{v\text{-}linear}$ and $\sigma_{v\text{-}parabolic}$ on the number of measured frequency points N around the BFS. As previously stated, the results will be compared theoretically and experimentally. The measurements are performed with 20 ns optical pump pulses, thus leading to a Brillouin linewidth $\Delta\nu_B$ of 56.7 MHz. The traces are averaged 300 times providing an equivalent SNR of 13.4 (11.3 dB). The experimental errors are obtained from the standard deviation calculated from a set of about 100 estimated BFSs at close positions, in a uniform fiber section, exactly as it was done in [4]. Figure 4 shows a representation of the quadratic and linear errors (experimental and theoretical for each case) for different frequency sampling steps (δ = 0.25, 0.5, 1.5, 2, and 3 MHz). As long as the sampling step increases, the numbers of points effectively used to determine the error is consequently reduced (note that the number of points used in the fittings is in all cases bounded to a region of $\Delta\nu_B$ around the BFS, as required by Eq. (11)).

As can be observed, for an elevated number of sampling points (N > 100), and consequently a small sampling step ($\delta \leq$ 0.5 MHz), the error in both cases remains below 1 MHz and perfectly fits with the theoretical tendency. When N is reduced, the fitting spectral range concentrates around the central frequency and the error rapidly increases for the quadratic case, in agreement with the prediction and the results reported in [4]. In contrast, for the linear case, the error remains quite bounded for nearly all values of N (note that for N < 10 the results may not be statistically significant enough). For both cases, the experimental error matches fairly well the theoretical error. Bearing in mind that the linear fitting is only possible considering measurement points within the FWHM of the BGS (linear region of the BPS), hence $(N\text{-}1)\delta < \Delta\nu_B$, the number of points cannot be very high for large sampling steps ($\delta \geq$ 1.5 MHz).

Optics EXPRESS

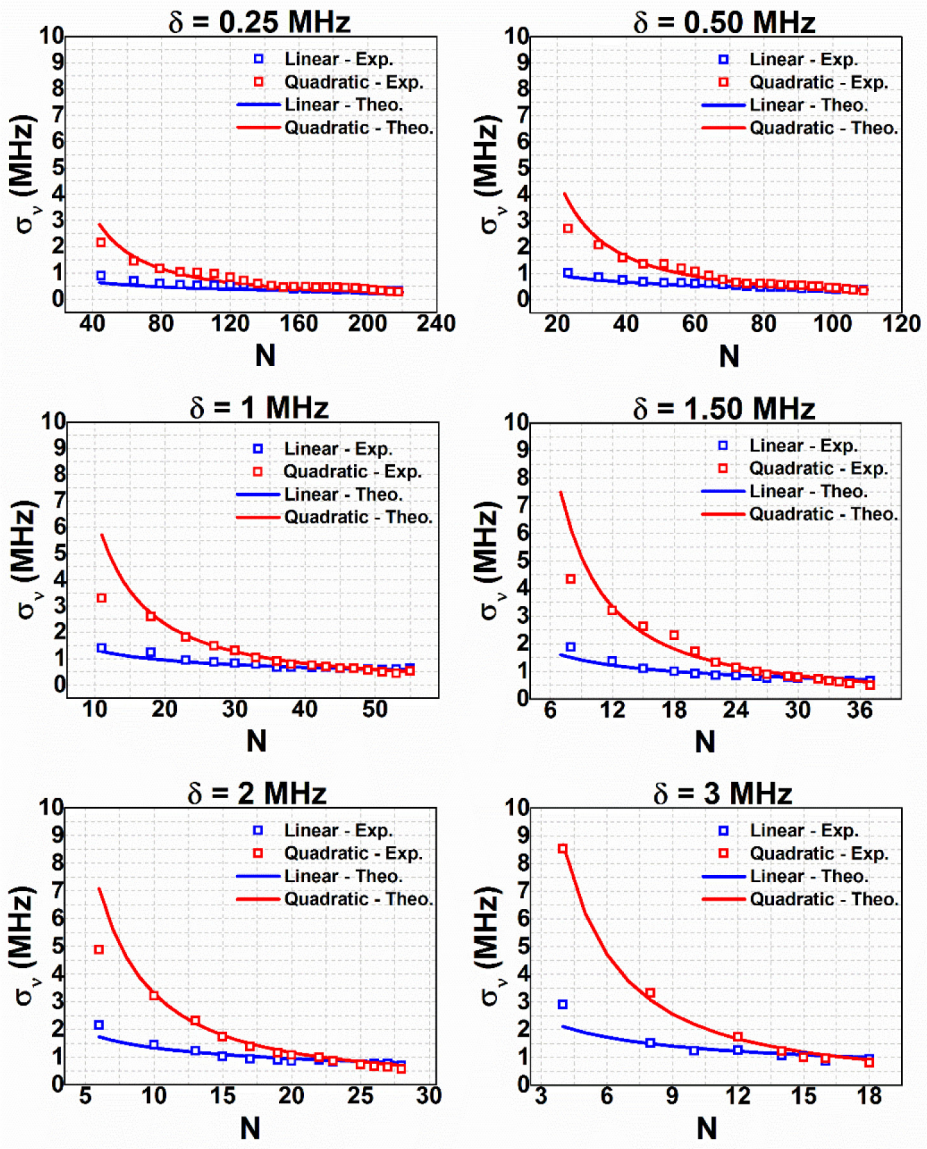

Fig. 4. Linear and quadratic BFS determination error vs. the number of fitting points. The analysis has been performed for different frequency sampling steps (δ = 0.25, 0.5, 1, 1.5, 2, and 3 MHz), with experimental results retrieved with 20 ns pulses and a 13.4 SNR equivalent to 300 average number. The results show theoretical simulations as well as experimental results. In all the cases, the highest N corresponds to the use of the full $\Delta\nu_B$ frequency range around the BFS position.

Considering Eqs. (8) and (11), if we represent both errors as a function of the sampling step δ for a constant N, the error in the linear fitting case will in principle experience no variations, as it is not affected by this variable, while the quadratic fit should deteriorate with smaller steps since the points concentrate more in the central part of the spectral profile. Figure 5 shows the cited representation for the particular case of a spectral width of 56.7 MHz (20 ns optical pulses) and N = 18 points. This particular number of points has been selected in order to be able to represent all the acquired sampling steps for the particular $\Delta\nu_B$ used. As it can be seen, the evolution of the error using the linear fit remains basically constant for

Optics EXPRESS

frequency sampling steps greater than 0.5 MHz, i.e. when the fitted spectral range is higher than 9 MHz (representing a $\xi \approx 0.16$). For sampling steps smaller than 0.5 MHz, the offsets in the centering (vertical and horizontal) become non-negligible and have an increasing influence in the error as shown by Eq. (6). In addition, the relative noise amplitude becomes too big with respect to the peak-to-peak amplitude response (max-min of the phase amplitude is too small in comparison to the noise). The quadratic fitting shows an inverse dependence with the frequency step in both the theoretical expectation and the experimental points. In this particular situation, for sampling steps greater than 3 MHz, the quadratic fit of the BGS will provide lower error than the linear approach since the points cover most of the gain spectral FWHM.

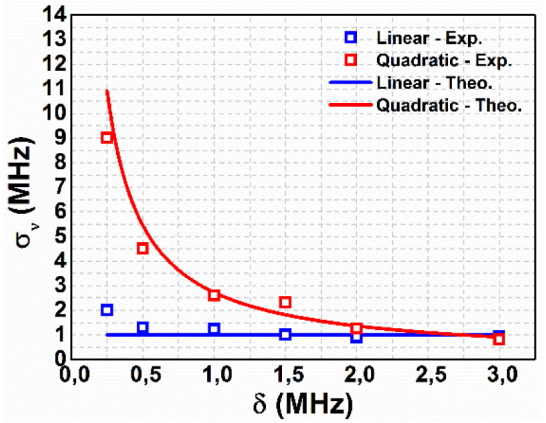

Fig. 5. Error comparison as a function of δ for 20 ns pulses ($\Delta\nu_B$ = 56.7 MHz) and N = 18. As observed, the linear error has no basic dependence upon the sampling step, as predicted by Eq. (8).

To check the dependence on another quantity, the error achieved when fitting the retrieved experimental gain or phase traces as a function of the gain spectral linewidth $\Delta\nu_B$ is shown in Fig. 6. As long as the optical pump pulse width is reduced, the spectral width of the SBS process is increased. Higher $\Delta\nu_B$ typically leads to greater error when determining the BFS as the response broadens. For our particular case we employed optical pulses of 60, 30, 20 and 10 ns which led to spectral linewidths of 35.3, 39.3, 57.9 and 90.0 MHz respectively. We set a constant fitting range with a fixed sampling step δ again to 1 MHz, a fixed number of fitting points N to 35 and assured the SNR of each measurement to be 10.6 (10.3 dB).

As in all the previous cases, the obtained results show good match with the expressions (8) and (11). For the quadratic error case, as represented, the error grows faster with $\Delta\nu_B$ since the points condense in the central spectral region, as indicated by the quadratic dependence in Eq. (11). On the contrary, in the linear case the error tendency is linear with $\Delta\nu_B$. As it can be seen, for the particular case of 30 ns pump pulses (39.3 MHz spectral width) the performance of quadratic and linear errors is similar. If longer pump pulses are employed (the spectral width $\Delta\nu_B$ is reduced), the quadratic error suits better the determination of the BFS while if the pulse is narrower (leading to a broadened spectrum) the error rapidly increases, particularly in the quadratic fitting case, making the linear fit more attractive in these conditions of points concentrated in the central region.

Optics EXPRESS

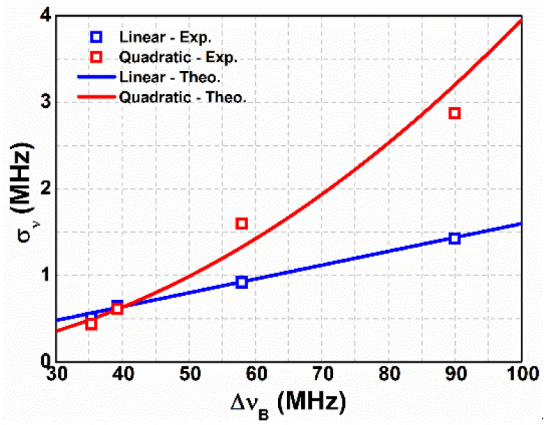

Fig. 6. Linear and quadratic BFS determination error vs $\Delta\nu_B$. The analysis has been performed for δ = 1 MHz, N = 35, and a SNR of 10.6. It is compatible with the quadratic tendency in the quadratic error while the linear fit trend follows a straight line.

Once the error introduced by both linear and quadratic fits has been evaluated versus the number of fitting points and frequency step, it is possible to evaluate how both types of fitting procedures behave as a function of the SNR. The results are represented in Fig. 7 and have been experimentally obtained by varying the number of averages on the measured traces to consequently modify the SNR from 4.1 (6.1 dB) up to 13.4 (11.3 dB). For all measurements, 20 ns optical pump pulses ($\Delta\nu_B$ = 56.7 MHz), a frequency step δ of 1 MHz, and a number of sampling points N of 44, were employed. The number of fitting points has been selected in order to perform a fair comparison among both fitting techniques, by setting a fitting spectral range a bit narrower than $\Delta\nu_B$, so that both fittings are expected to perform almost identically.

As can be seen, both fitting procedures follow the same inverse dependence with the SNR in accordance with Eqs. (8) and (11). The described representation shows good match between the theoretical and experimental results, for both quadratic and linear fits. Results show that, as long as the SNR remains elevated enough (≥ 9, equivalent to 9.5 dB), an error close to 1 MHz can be maintained. If the SNR is set below, the introduced error increases and rapidly surpasses 1.5 MHz.

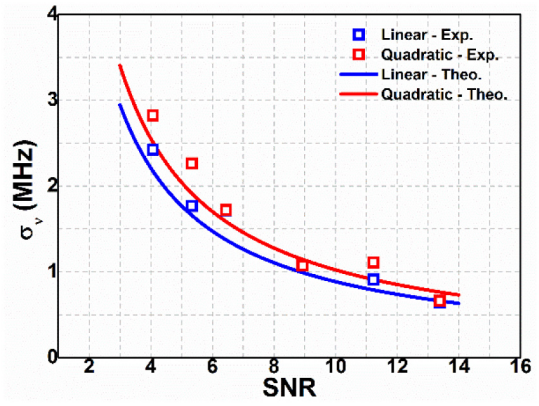

Fig. 7. Linear and quadratic BFS determination error vs. SNR. The analysis has been performed with 20 ns pulses, a δ = 1 MHz and N = 44.

After having experimentally verified Eqs. (8) and (11) as a function of the different parameters involved, it turns out interesting to compare when the use of linear or quadratic

Optics EXPRESS

fitting should be preferable. If a ratio among Eqs. (8) and (11) is performed, the following expression can be obtained:

$$\frac{\sigma_{\nu-parabolic}(z)}{\sigma_{\nu-linear}(z)} = \frac{\sqrt{3}}{2\xi} \tag{12}$$

As it can be seen in this expression, when the normalized fitted spectral span ξ decreases, the linear fitting of the BPS becomes favored (as suggested by the initial intuition). When the ratio in Eq. (12) is larger than 1, it means that the linear fitting of the BPS should be preferred. This condition is fulfilled when the normalized measurement span ($\xi = N\,\delta/\Delta\nu_B$), is smaller than $\sqrt{3}/2$ (or 0.87). In case of employing an incremental fitting (in which the span used in the determination is progressively increased along the measurement), when just a few number of sampling points N is selected, the BFS estimation will be better in the beginning utilizing the linear fit over the BPS profile. As the number of frequencies N is increased, the use of the quadratic fit over the BGS would become preferable. Figure 8 represents this ratio for the particular case of a constant sampling step of 1 MHz and a Brillouin linewidth of 56.7 MHz. It can be seen that the error ratio fits, broadly speaking, the expected decreasing tendency with the measured span. The experimental results included in Fig. 8 are for the particular case of using a frequency sampling step equal to 1 MHz. This situation determines that the transition between the two cases is produced when the spectral measurement span used in the fitting is around 49 MHz, corresponding to about 86% of the gain FWHM. It is therefore evident that, depending on the application and the necessary spectral sweep performed, one or the other fitting procedure may be used more conveniently. Anyway, simply evaluating the expression given in Eq. (12) might be a simple way to determine which methodology is more appropriate. As a general tendency, considering that most of BOTDA applications need to perform a wide frequency sweep to cover a broad measurand range, a large value of ξ will normally be available, which benefits the quadratic fit. However, in some specific applications where small frequency sweeps could be feasible (homogeneous fibers, dynamic systems), the linear fit could be a better choice.

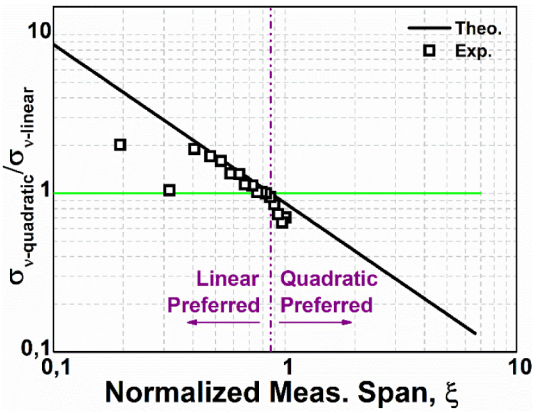

Fig. 8. Logarithmic representation of the ratio among quadratic and linear errors as a function of ξ when δ = 1 MHz and $\Delta\nu_B$ = 56.7 MHz. As can be seen, for ξ values greater than $\sqrt{3}/2$, the quadratic fit suits better. This condition is generally fulfilled for standard frequency sweeps, when the tested number of frequencies is around two times the $\Delta\nu_B$ of the system.

Based on the obtained results, we can consider that the theoretical expressions retrieved in Eqs. (8) and (11) have been validated by experimentally testing them when one basic parameter is varied. But to make a meaningful comparison, it may be helpful to reformulate Eqs. (8) and (11) to highlight the dependence on experimental conditions as observed in a real

Optics EXPRESS

situation. When practically performing a measurement of the Brillouin spectral response, a certain granularity for the frequency scan is chosen, so that the frequency step δ is set to a fraction of the Brillouin gain linewidth $\Delta\nu_B$. This is mostly dictated by the overall measurement time and the targeted final precision on the determination of the BFS. After acquiring the data, the fitting procedure is performed over a frequency span that is also a fraction of the Brillouin gain linewidth $\Delta\nu_B$, properly defined by the normalized frequency span ξ as given in Eq. (10). Using this approach Eqs. (8) and (11) can be reformulated into the following expressions:

$$\sigma_{\nu-linear}(z) = \sigma(z)\Delta\nu_B \frac{1}{\sqrt{\xi}}\sqrt{\frac{\delta}{\Delta\nu_B}} \tag{13}$$

$$\sigma_{\nu-parabolic}(z) = \sigma(z)\Delta\nu_B \sqrt{\frac{3}{4\xi^3}}\sqrt{\frac{\delta}{\Delta\nu_B}} \tag{14}$$

The errors now show a very similar functional relationship with the measurement parameters and only differ by their dependence on the normalized frequency span ξ, which is much stronger in the quadratic case. This simply confirms what was observed intuitively, theoretically and in the experimental validation and reflects the fact that the central region of the spectral profile gives estimations with maximum error for the BGS and minimum error for the BPS. However, this also shows that the errors are fairly similar in both cases when ξ is close to 1, since points with larger variations are now included in the fitting range for the quadratic case and both estimations turn equally precise.

This comparative analysis leads to the simple observation that the linear approach behaves better when the measured span is small in comparison to the FWHM region of the BGS ($N\delta < \sqrt{3}\Delta\nu_B/2$). This could be highly beneficial for particular applications where fast measurements are required over very uniform fibers. However, in the case where the BGS is measured using a standard procedure, when a full coverage of the Brillouin spectral response is realized, then the quadratic fitting becomes more appropriate regarding its slightly better accuracy and, more importantly, its intrinsic immunity to vertical offset inaccuracy. In any case, it is possible to optimize the quadratic fit by properly selecting the measurement parameters to fit over a normalized spectral span (ξ parameter) larger than $\sqrt{3}/2$. This condition is nevertheless quite usual in robust BOTDA systems requiring a large enough measurement span to cope with the fiber inhomogeneities and large variations of the ambient parameters.

Interestingly, the possibility of combining BFS profiles obtained from simultaneous and independent BGS and BPS measurements might provide the advantage of redundant measurements, which could increase the effectiveness of the system in terms of sensing accuracy. If each spectrum (BGS and BPS) presents independent noise, the combination (averaging) of both BFS profiles might reduce the uncertainly in the BFS determination by a factor of $\sqrt{2}$. In case of correlated noise in the BGS and BPS spectra (as in [12]), the combination of both determinations does not, in principle, provide such an important advantage over using just one of the two curves.

Optics EXPRESS

5. Conclusions

In conclusion, we have evaluated theoretically and experimentally the performance of the SBS phase response for BFS determination in distributed Brillouin sensors as a function of the different experimental parameters (number of sampling points, SNR, sampling step and spectral width). To the best of our knowledge, this is the first time this study is performed. To obtain the BFS from the BPS profile the simplest way is to perform a linear fit around the zero de-phase point of the SBS interaction. The performance of this methodology has been theoretically and experimentally tested and compared to the well-known quadratic fitting of the BGS. The proposed experimental comparison is based on results obtained using the Sagnac interferometer-based BOTDA presented in [9–12], which ensures the same SNR figure in both BGS and BPS measurements, making the comparison feasible and reliable.

The obtained theoretical expectation shows that the linear fit used for the BPS profile performs better than the conventional quadratic one used for BGS measurements when the measured spectral span is concentrated in the center of the spectral profile ($N\delta < \sqrt{3}\Delta\nu_B / 2$). However, these measuring conditions are not possible in all scenarios, as they would typically involve the need of a high-resolution setup and a homogeneous fiber with small BFS variations. Typically, for a robust sweep demanded in most applications, a measurement over a wide spectral range would be required, favoring the use of the quadratic fit. The adequateness of each technique can be easily determined by evaluating the normalized spectral span (ξ parameter $N\,\delta/\Delta\nu_B$) where the limit is set by the $\sqrt{3}/2$ factor. For values of $\xi > \sqrt{3}/2$ the quadratic fit should be preferred.

An example to illustrate the improvement given by the linear fit for small spectral spans is given for a rapid comparison: for a $\Delta\nu_B$ of 56.7 MHz (20 ns optical pump pulses), a sampling step of 1 MHz, and a SNR of 13.4 (11.3 dB), which are fairly standard measurement conditions, with a value of N = 18 ($N\,\delta/\Delta\nu_B$ = 0.32), the linear fit introduced a frequency determination error close to 1.4 MHz (acceptable for many applications) while the quadratic fit case in the same experimental conditions gave an error of around 2.6 MHz.

It is clear that the BPS response is still under-explored for sensing applications. Considering the above conclusions, we believe that the BPS measurement may open the way to achieving a reduced measurement time in certain distributed Brillouin sensors, by simply reducing the spectral range required to achieve the same BFS determination error. This is clearly an important aspect to be explored in the future. However, our final comparative expressions show that there is no decisively better technique in normal situations and for a given SNR the precision on the determination of the BFS will be essentially similar, in both cases, assuming no offset in the measurements. In addition, it can be confidently stated that the quadratic fit is more robust, regarding the intrinsic sensitivity of the phase response to any residual offset. It can be then concluded that the efforts have to be preferably placed on techniques giving a SNR as large as possible, rather than speculating on a fitting strategy.

Funding

ERC (Grant 307441); Spanish "Plan Nacional de I+D+i" (TEC2013-45265-R, TEC2015-71127C2-2-R); Comunidad de Madrid (SINFOTON-CM: S2013/MIT-2790). European Commission (Horizon 2020) and MINECO, Spain, under the ERA-NET Cofund WaterWork2014 call (Water JPI, project DOMINO).

Acknowledgments

S. Martin-Lopez acknowledges support from the Spanish "Ministerio de Economía y Competitividad" through a "Ramón y Cajal" contract.